Textile UHF-RFID Antenna Embroidered on Surgical Masks for Future Textile Sensing Applications

Chengyang Luo, *Member, IEEE,* Ignacio Gil, and Raúl Fernández-García

***Abstract*—Ultra High Frequency (UHF, 865-868 MHz) Radio Frequency Identification (RFID) devices are expected to be implemented in many health-caring areas. In this paper, we present three progressive designs of textile UHF-RFID antennas on surgical masks using a function-extensible integrated circuit (IC) chip (Rocky 100). The simulated and measured resonance curves of the designs all match well ($|S_{11}| <$ -20 dB at 868 MHz) and the maximum realized gain are improved progressively in order to overcome the difficulty of the chip low sensitivity and increase the maximum read range. The best type (Design 3) is selected and its read range measured by the RFID reader (M6e kit) can reach 2.5 m in air. In addition, several reliability validation measurements are performed, such as bending and skin contact, and maximum read range can reach 1.1 m considering the on-body worn worst case. The proposed Design 3 allows common use as a tag for tracking or safe distance alert under an epidemic situation. Alternatively, for the used function-extensible chip, the design can be applied to many different types of sensors for various application scenarios.**

***Index Terms*—Textile, Ultra High Frequency Radio Frequency Identification (UHF-RFID), textile antenna, conductive yarns, surgical masks, bending, skin contact, backscattering, read range, Rocky 100, M6e kit**

I. Introduction

In modern society, Radio Frequency Identification (RFID) technology is essential in diverse applications [1] [2] [3] such as the goods classification, industrial process monitoring [4], transportation [5], localization and stuff management [6]. Most of them are developed on a hard or flexible Printed Circuit Board (PCB) with popular circuit (IC) chips such as EM4237SLIC, SL3S5002N0FUD and Monza R6. In addition, some tags can be designed to connect sensors with different functions [7]. For these types of RFID sensors, IC chips need to have extendable ports for sensors connection and optional power interface. Compared with the common Ultra High Frequency (UHF, 865-868 MHz) RFID tags and sensors on PCB, the majority of textile UHF-RFID tags and sensors are embroidered by conductive yarns on textile substrates [2] [8], which is different with the copper on PCB. On the one hand, the textile tags can be developed on common clothes which are more comfortable and lighter than those based on PCB inserted into clothes. On the other hand, the conductive yarns and textile substrates are sensitive to the environmental factors such as humidity [9], temperature, bending and washing [10] [11]. As a result, before addressing the electromagnetic simulation design, the parameters of the materials such as permittivity, loss tangent and thickness need to be confirmed. After the designs are embroidered, related reliability tests need to be operated.

Some textile RFID tags and sensors are designed with two-pad IC chips which are small and more sensitive to wake up. However, these types of chips with two pads and low wake-up power are especially used as ID textile tags [14]. The related sensing functions can be only explored by the features of textile materials, which limits the sensing applications. For example, the textile antenna (Bellyband antenna) [16] designed with the IC chip Murata Magicstrap LMXS31ACNA-011 is used as a tag with a strain sensing function. In addition, there is no other interface for extensional sensing functions and on-body read range is only 0.6 m [18]. As a result, exploring the possibility and reliability of the function-extensible IC chips is also a novel research orientation.

Moreover, for the special features of textile materials [12], related UHF-RFID tags and sensors for health-caring monitoring [13] [14] and diagnosis [15] are of growing concern in recent years. Most of them are used in health-caring applications such as breath monitoring for pregnant women or babies [16], move tracking for patients [19] and temperature monitoring. However, for the future aging society and Internet of Things (IOT) development, novel applications for health-caring areas based on textile UHF-RFID sensing technology are expected to be explored and related challenges such as the function-extensible IC chips used on textile materials need to be overcome.

In this paper, considering a general epidemic situation in which the surgical masks are frequently used for human beings protection, we develop three progressive designs of textile UHF-RFID antennas on surgical masks and the used IC chip (Rocky 100) is extensible for different sensors. Related preparatory work before simulation such as the permittivity, loss tangent, thickness measurements and detailed embroidery method is implemented and presented. We explain the progress of the three designs through comparison between their simulated resonance and radiation performance. For the measurements of the impedance and read range, we compare the results to the electromagnetic simulations to validate their performance. Finally, we apply the selected sample to

Manuscript received Month DD, YYYY; revised Month DD, YYYY; accepted Month DD, YYYY. This work was supported in part by Spanish Government-MINECO under Project TEC2016-79465-R, and China Scholarship Council under Grant No.201908440233. Corresponding authors: Raúl Fernández-García.

The authors are with Department of Electronic Engineering, Universitat Politecnica de Catalunya, Barcelona 08222, Spain (e-mail: raul.fernandez-garcia@upc.edu; chengyang.luo@upc.edu).

validate the reliability by the tests under bending and skin-contact situations. The basic use of the designs is the user identification, Nevertheless, due to the function extensibility of the chips, various textile sensors can be included under specific scenarios.

II. Design and Related Work

A. Progressive textile UHF-RFID designs

The textile UHF-RFID antennas are designed on surgical masks and the configuration of the proposed progressive designs are shown in Fig.1. Considering the used chip (Rocky 100) with a capacitive impedance of 64-i*469 ohm, the proposed antennas are expected to be designed with an inductive behavior. Note that for UHF-RFID chips with complex impedance, the corresponding antenna design way is different from conventional antenna design experience (such as W11<<L11 for a conventional folded dipole) with a feed port of 50 ohm. Therefore, a loop structure for matching as shown in Fig. 1 (a) has been selected as a design strategy. Then through an electromagnetic field analysis as illustrated in next section and typical 'T-match' structure analysis [17], the progressive structures, Design 2 and 3 are developed as shown in Fig. 1 (b) and (c), respectively. As a consequence, the Design 3 is derived from the simple 'T-match' structure with 'circular end caps' for increasing the radiation property (directivity and realized gain). The size parameters are detailed in Table I. All of the designs are embroidered using conductive yarns as antennas and surgical masks as substrates. The textile material of the antennas is a commercial conductive twisted yarn (Shieldex 117/17 dtex 2-ply) made of 99% pure silver-plated Nylon (bulk conductivity: 11500 siemens/m). Moreover, as shown in Fig. 1 (c), the UHF-RFID chip (Rocky 100) is sewed by Nylon yarn which is not conductive and fixed by a type of glue (G-15). The substrate is a type of common surgical masks made of staple fibres (short) and long fibres (continuous long).

Due to the non-rigid geometry of the surgical mask and its electrical parameters such as permittivity (ε_r) and loss tangent ($tan\theta$), the surgical mask has an effect on the UHF-RFID antenna performance. In addition, ε_r and $tan\theta$ are two essential parameters for simulation and in order to obtain more accurate values, the two parameters of the masks (ε_r: 1.1439 and $tan\theta$: 0.0001265) are measured by a split post dielectric resonator with a Microwave Frequency Q-Meter as shown in Fig. 2. On the other hand, its thickness ($Thic_r$ = 0.62 mm) can be measured by the Electronics Outside Micrometer (132-01-040A) which has 0 - 25 mm read range and 0.001 mm resolution of digit.

TABLE I
Size Parameters of the Designs (Unit: mm)

$Type$	L_{11}	W_{11}	T_{11}		
$Design\ 1$	34	21	2		
$Type$	L_{21}	L_{22}	W_{21}	T_{21}	
$Design\ 2$	33	22	20	2	
$Type$	L_{31}	L_{32}	W_{31}	T_{31}	R_{31}
$Design\ 3$	27	20	20	2	10

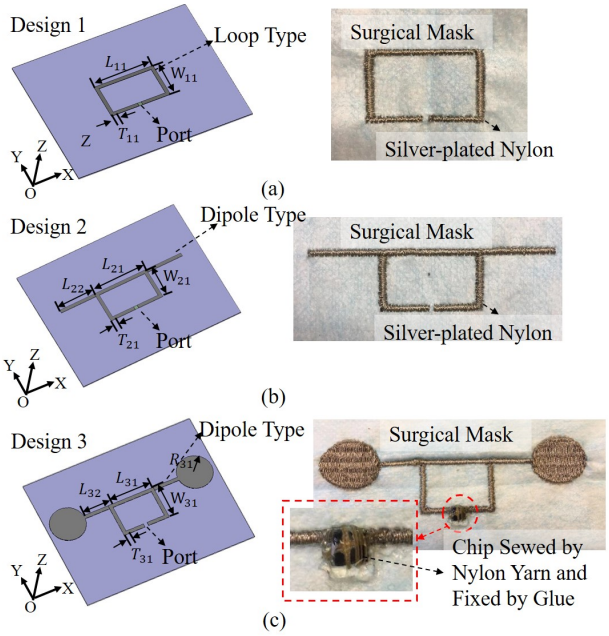

Fig. 1. Configuration of the proposed progressive designs. (a)loop type, (b) dipole type with balanced 'arms', (c) dipole type with balanced 'circular end caps'.

In addition, note that the UHF-RFID chip (Rocky 100) is selected for the work, which is different from the chips used in most textile/knitted wearable UHF-RFID tags. The Rocky 100 chip is normally used for UHF-RFID sensors on PCB. In other words, this chip has several pads (16 pads) which can be used for sensors connection in active/passive situations for many different sensing applications. Compared with some popular chips such as Monza R6 with two pads, the Rocky 100 has a lower sensitivity (minimum wake-up power) of -10 dBm, while Monza R6 has higher sensitivity of about -20 dBm. As a result, the UHF-RFID antenna needs to be designed for higher gain and good conjugate impedance match with the chip.

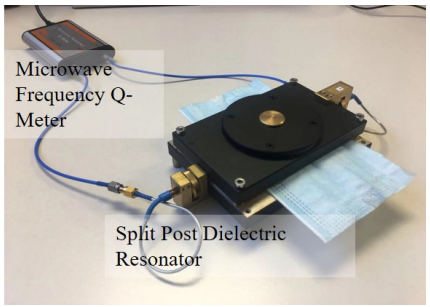

Fig. 2. Substrate permittivity and loss tangent measurements.

B. Method for Impedance Measurements

For balanced antennas, a popular method for impedance measurements is to combine the function (port extension) of the Microwave Analyzer (N9916A) with the common-earth cables as shown in Fig. 3. This method was validated in some

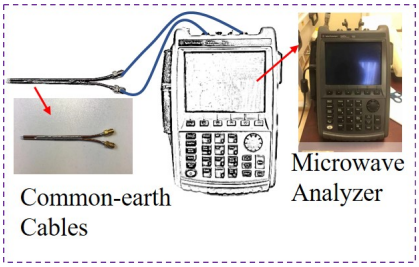

Fig. 3. Calibration setup with the common-earth cables for impedance measurements method.

works [20] [21] [22]. Concerning to the procedure, first of all, the Microwave Analyzer with two professional cables needs to be calibrated by a standard calibration kit. Secondly, after connecting the professional cables to the common-earth cables, the function (port extension) of the Microwave Analyzer needs to be adjusted in order to move the calibration plane from the ends of the professional cables to the ends of the common-earth cables. And then, the traces in smith chart of the two ports should roughly converge to the open circuit position in Microwave Analyzer.. Next, the two tips of the common-earth cables are connected to the proposed textile UHF-RFID antennas and the S parameters in 50 ohms can be obtained. Note that the measured S parameters using the common-earth cables are earth-referenced and need to be transferred for the differential reflection coefficient (ρ) of the antennas. Finally, Z parameters of the tested antennas and the differential reflection coefficient (ρ) in the complex conjugate impedance of the chip can be calculated using the equations 1 and 2 as follows,

$$Z_{ant} = \frac{2Z_0(1 - S_{11}S_{22} + S_{12}S_{21} - S_{12} - S_{21})}{(1 - S_{11})(1 - S_{22}) - S_{12}S_{21}} \quad (1)$$

Where Z_0 is 50 ohms, S_{11}, S_{12}, S_{21} and S_{22} are the measured S parameters, Z_{ant} is the Z parameters of the tested antennas. And,

$$\rho = \frac{Z_{ant} - Z^*_{chip}}{Z_{ant} + Z^*_{chip}} \quad (2)$$

Where Z^*_{chip} is the conjugate impedance(64+i*469) of the chip and ρ is the differential reflection coefficient (also called S_{11}) in the complex conjugate impedance of the chip.

III. Simulation and Analysis

Considering that the complex impedance of the used chip (Rocky 100) is 64-i*469 ohm, the impedance of the designed antenna should be close to 64+i*469 ohm. Note that the chip has higher resistance and reactance than that of some two-pad UHF-RFID chips such as the Monza R6 with the complex impedance of 12-i*120 ohm. In some antenna designs, resistance and reactance curves for antennas present fast-changing slopes and larger tangent, which means that the resistance and reactance values change sensitively. Hence in order to reduce the effects on frequency bandwidth of antenna designs, it is more important that the designed antenna can have a good conjugate impedance match with the chip [23] [24], which implies that the designed antennas need to have complex impedance with the conjugate impedance of the chip as close as possible. In addition, the differential reflection coefficient (ρ) of the work band should be lower than -10 dB.

In addition, as mentioned in previous section, although the function-extensible feature of the chip (Rocky 100) is attractive, its lower sensitivity still needs to be considered. Therefore, the UHF-RFID antenna needs to be designed to achieve a realized gain as high as possible (at least higher than -3 dBi). For the proposed three designs, one of the targets is to improve the gain but reduce the impact on the conjugate impedance match. As a results, the Design 1, 2 and 3 are optimized progressively. After being optimized, the three designs are shown in Fig.1 and the final size parameters are shown in Table I.

A. Resonance Analysis

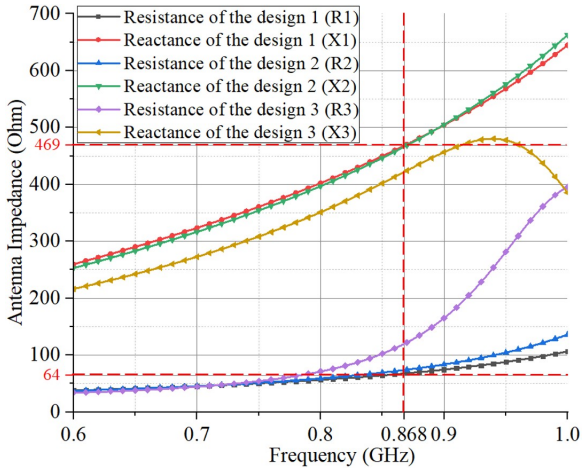

Fig. 4. Simulated impedance for the three progressive designs (Dashed lines: required antenna complex impedance 64+i*469 ohm at 868 MHz).

Fig. 4 shows the simulated impedance for the three progressive designs, including the resistance and reactance curves. The three designs behave inductively at the resonance frequency (868 MHz), in which the closer two to the feed impedance are the Design 1 and 2 with impedance of 67+i*468 ohm and 74+i*466 ohm, respectively. The Design 2 can be developed by a size-optimized Design 1 with balanced 'arms'. By adding the circular end caps to the Design 2 and optimizing the size parameters, Design 3 has impedance of 119+i*421 ohm. Although the impedance match seems to degrade from Design 1 to 3, the reflection coefficients of the three designs as shown in Fig. 5 are still within acceptable limits. In addition, the 'arms' and the 'circular end caps' are expected to increase the antenna gain.

In detail, the S parameters (reflection coefficients) of the three designs as shown in Fig. 5 are all under the -10 dB at 868 MHz. At resonance point (868 MHz), the Design 1, 2 and 3 have reflection coefficients of -48 dB, -39 dB and -22 dB, respectively. The Design 1 and 2 present a bandwidth of at least 400 MHz (Design 1: 560 MHz and Design 2: 515 MHz), while Design 3 have a bandwidth of 370 MHz. In addition, transmission coefficients (τ) for the Design 1, 2 and 3 can be

calculated as 0.9992, 0.9945 and 0.8519, respectively. Due to the basic features of general textile materials, environmental factors often make influence on the resonance frequency of the textile UHF-RFID antennas. As a result, the bigger bandwidth can improve reliability when the resonance frequency shifts within a certain range.

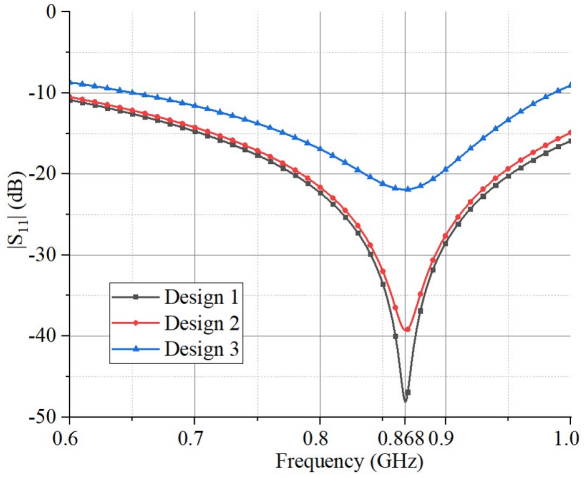

Fig. 5. Simulated reflection coefficients for the three progressive designs.

B. Radiation Performance Comparison

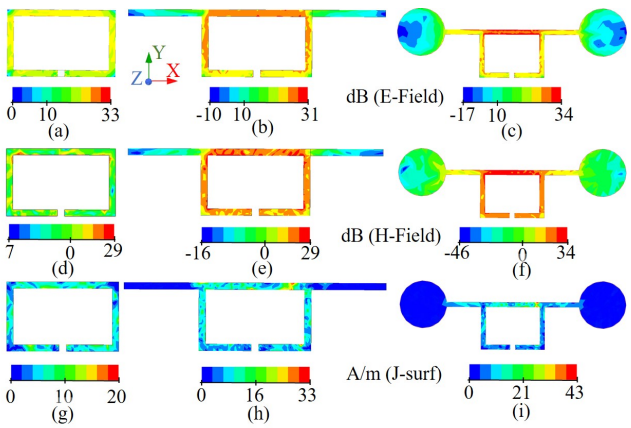

Fig. 6. Electromagnetic fields and current distribution at 868 MHz. Design1: (a), (d) and (g). Design 2: (b), (e) and (h). Design 3: (c), (f) and (i).

The electric field, magnetic field and current distribution at 868 MHz are shown in Fig. 6. It is found that from the Design 1 to the design 3, the electric fields and magnetic fields are raised and their distribution ranges are extended gradually after adding the 'arms' and 'circular end caps'and adjusting loop and 'arms' sizes. In addition, it is found that after adding arms and changing loop size, the overall fields and currents of the Design 1, 2 and 3 get stronger. From the aforementioned features, adjusting the loop and 'arms' can obtain required the frequency and changing the size of the 'circular end caps' can affect the radiation performance. Fig. 7 shows the radiation patterns in the xoy cut for the three designs. The structure of the Design 1 is only a loop which means the radiation ability is weak. For increasing the radiation ability (realized gain), the 'arms' can be added into the structure as the Design 2 which also make an impact on the impedance. From the current distribution as shown in Fig. 6, the realized gain of the Design 3 is expected to be higher than that of the previous designs. As shown in Fig. 7, the peak realized gain values of the three designs are -10.86 dBi, -7.87 dBi and 1.09 dBi, respectively. In addition, from the H-plane (yoz cut) as shown in Fig. 7 (b), the proposed Design 3 has a dipole-like radiation pattern as expected.

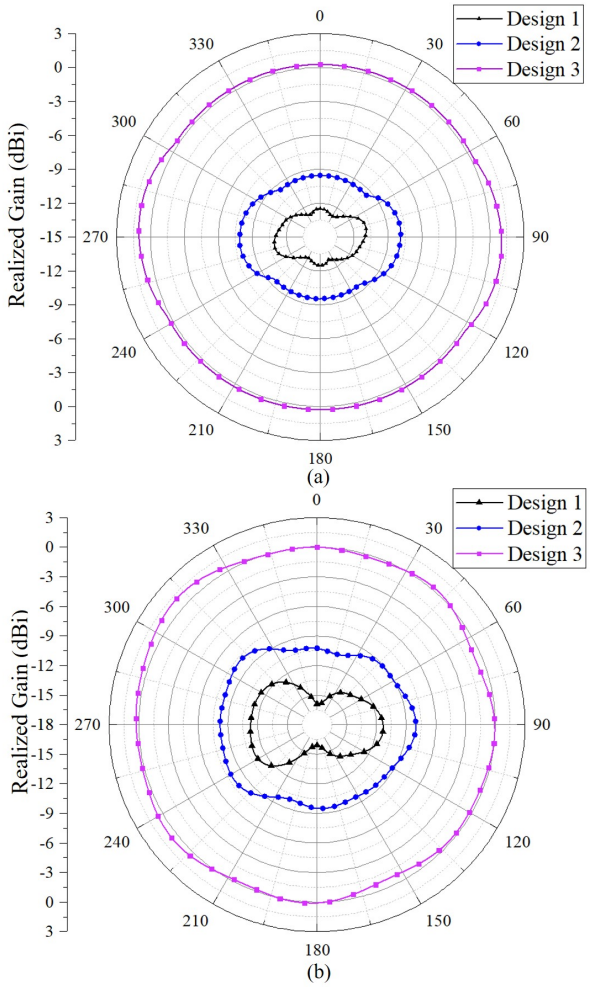

Fig. 7. Simulated normalized radiation patterns ~~(normalized realized gain)~~ for the three progressive designs (a) xoy cut, (b) yoz cut.

IV. Manufacture and Test

A. Embroidery Method

To embroider the patterns on the substrate (surgical masks), a professional embroidery machine (Singer Futura XL-550) is used. For the embroidery procedure as shown in Fig. 8, some details need attention. First of all, after obtaining appropriate designs in simulation software (ADS momentum, CST and HFSS), the simulated models need to be exported to a type of formats which can be converted with same size into the related embroidery software. Secondly, the knit pattern size and boundaries of the designs affected slightly by embroidery

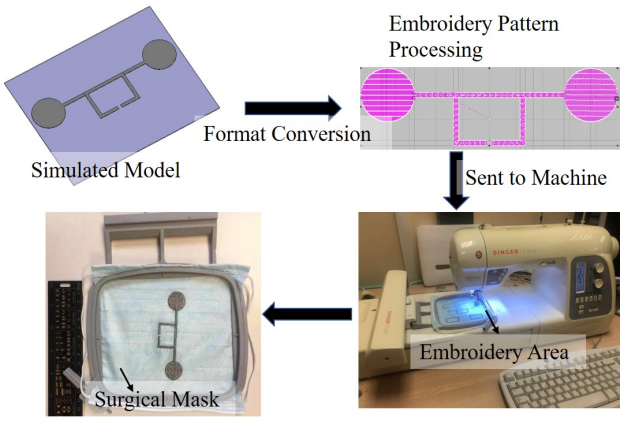

Fig. 8. Embroidery procedure.

modes in the embroidery software (EasyDesign EX4.0) need to be adjusted carefully, which is a factor affecting real conductivity of the conductive yarns. For the proposed designs, the 'satin fill' mode in the embroidery software is adopted. Finally, in the manufacturing process, the proposed yarn is utilized in both sides of the substrate as the conductive yarn and support yarn for reducing the influence from other dielectric yarns as support yarn.

B. Impedance Tests

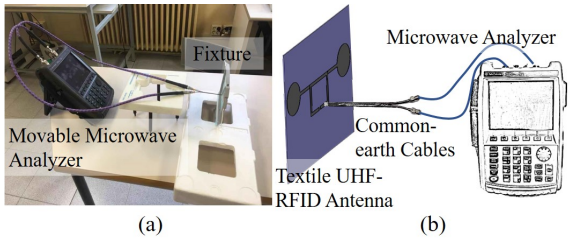

Fig. 9. Measurement setup for the impedance and reflection coefficients of the embroidered designs. (a) Photograph of measurement setup, (b) Measurement setup configuration.

For the measurements of the impedance and reflection coefficients of the embroidered designs, the experimental setup is shown in Fig. 9. As mentioned in section II, the common-earth cables are added at the end of the two ports and the related differential measurement method is used. Fig. 10 shows the antenna impedance of the proposed simulated and measured Design 3, including the resistance part and the reactance part. It is found that the resistance parts are higher than 64 ohm and reactance parts are lower than 469 ohm. Certainly, analyzing all of the results, the measured curves are close to the simulated curves.

From equation 2, the reflection coefficient (S parameter) can be calculated as shown in Fig. 11. It is found that the $|S_{11}|$ of the measured Design 3 is -24 dB which is better than the simulated results at 868 MHz. Note that the Design 3 have slight difference of the resonance frequency shift degrees between the simulated and measured results (below 10 MHz).

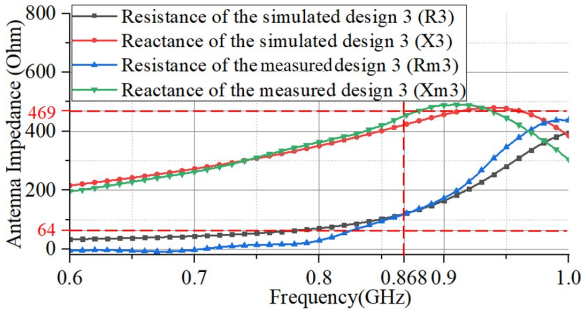

Fig. 10. Simulated and measured impedance for the embroidered Design 3 (Dashed lines: required antenna complex impedance 64+i*469 ohm at 868 MHz).

In addition, the Design 3 have narrower bandwidths of about than that of the simulated designs.

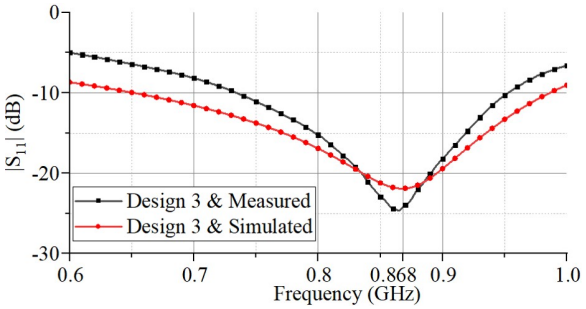

Fig. 11. Simulated and measured reflection coefficients for the embroidered Design 3.

C. Read Range Tests

Considering the real use conditions of the proposed textile UHF-RFID tag on surgical masks such as in the hospital channels and rooms, the read range measurement setup is shown in Fig. 12. The reader antenna (MT-242025/TRH/A/A) can be controlled by the M6E Kit which is connected to a laptop with control software. An inquiry signal with data and clock can be adjusted by the software and sent by the reader antenna. The proposed textile UHF-RFID antennas can send a backscattered signal with data and clock after receiving the inquiry signal. Note that backscattering coupling is a common mode in UHF RFID and Radar areas. In detail, when an electromagnetic wave encounters a space target, part of its energy is absorbed by the target, while the other part is scattered in various directions at different intensities. A portion of the scattered energy is reflected back to the transmitting antenna. [25]

When moving the proposed designs to a certain distance d as shown in Fig. 12 (b), the signal transmission is expected to be interrupted. This threshold distance is the maximum value of the read range.

To avoid moving the designs holders frequently, a certain distance is fixed (1 m) and then adjust the reader power to obtain the read range. In addition, the simulated read range can be calculated by the Friis Transmission Formula as follows,

$$d_{max} = \frac{\lambda}{4\pi}\sqrt{\frac{P_t G_t G_r \cdot \tau}{P_{th}}} \quad (3)$$

where d_{max} is the maximum value of the read range, λ is the wave length at 868 MHz, P_t is the power fed into the reader antenna, G_t is the gain of the reader antenna (7 dBi), G_r is the gain of the proposed antennas, τ is the largest power transmission coefficient and P_{th} is the minimum wake-up power of the chip (-10 dBm). In addition, the cable between the reader antenna and the reader have a loss of 0.8 dB.

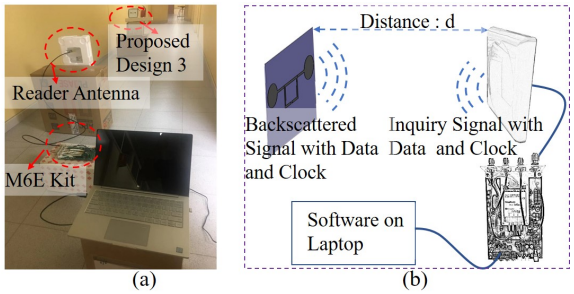

Fig. 12. Measurement setup for the read ranges of the embroidered designs. (a) Photograph of measurement setup, (b) Measurement setup configuration.

For the proposed designs, the read ranges are detected as shown in Table II. The maximum read range values of the simulated Design 1, 2 and 3 are 1.1 m, 1.6 m and 4.1 m, respectively, while that of the measured are 0.8 m, 1.3 m and 2.5 m, respectively. By analyzing the Friis Transmission Formula 3 and the proposed designs, the P_{th} of the chip (-10 dBm) makes a big impact on the maximum read range, compared to the two-pad chip (Monza R6) with the minimum wake-up power of -20 dBm. In addition, the difference between the simulated and measured results is caused by the silver-plated yarns and the soft substrates. In details, the silver-plated yarns are different with traditional copper line. The radiation ability of the yarns cannot be totally same with simulation results. For design 3, due to the soft masks, the 'circular end caps' has slight shape change in embroidery procedure which make a bigger difference between the simulated and measured results.

TABLE II
SIMULATED AND MEASURED MAXIMUM READ RANGE OF THE DESIGNS (UNIT: M)

Type	*Design* 1	*Design* 2	*Design* 3
Simulated d_{max}	1.1	1.6	4.1
Measured d_{max}	0.8	1.3	2.5

V. RELIABILITY VALIDATION

For textile UHF-RFID tags, reliability is an essential issue due to the features of the textile materials. In this work, considering the uses of surgical masks, the impact of bending and use on body is expected to be validated. In addition, with regard to the read range results at last section, the Design 3 is selected to be the final design which is tested for bending and skin touching.

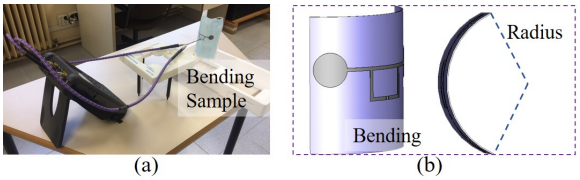

Fig. 13. Measurement setup for the impedance and reflection coefficients of the embroidered designs. (a) Photograph of measurement setup, (b) Diagram of the bending orientation.

A. Bending

The bending test setup is shown in Fig. 13 (a). Several molds with different radius have been used for hold and keep the proposed sample bent. Considering the use of surgical masks, the bending orientation is fixed as shown in Fig. 13 (b). Note that the bending degree increases with decreasing radius. Fig. 14 shows the measured antenna impedance curves in different radius. From Fig. 14, the resistance values at 868 MHz are close with different radius while the reactance values at 868 MHz increase with decreasing radius. In addition, the reflection coefficient curves as shown in Fig. 15 have slight resonance frequency shift degrees (all below 20 MHz) and increasing $|S_{11}|$ values at 868 MHz with increasing bending degree. In other words, after bending in certain degrees (radius: 33 mm to the flat), the proposed textile UHF-RFID tag can still work well.

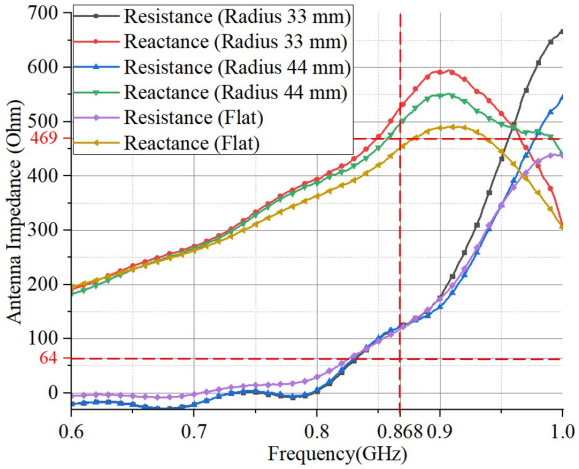

Fig. 14. Measured impedance in different bending degrees (Dashed lines: required antenna complex impedance 64+i*469 ohm at 868 MHz).

Certainly, read range tests in different bending degrees are still important and the test configuration is shown in Fig. 12. Considering the real use of the proposed design is on face, the bending radius close to face sizes (33 mm and 44 mm) are chosen. The measured max values of the read ranges shown in Table III are 2.5 m, 2.2 m and 1.7 m at flat, bending radius 33 mm and bending radius 44 mm, respectively. Note that the measured max values are obtained by the proposed design facing to the reader antenna as shown in Fig. 11. From the results, increasing bending degrees (radius: flat to 33 mm) cause a decrease in read ranges and the minimum read range in bending is at least 1.7 m.

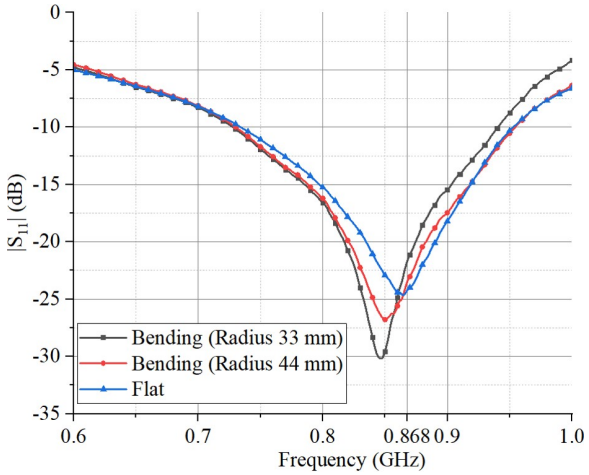

Fig. 15. Measured reflection coefficients in different bending degrees.

TABLE III
MEASURED MAXIMUM READ RANGE OF THE DESIGN 3 IN BENDING SITUATION (UNIT: M)

Type	*Flat*	*Bending*(0.044)	*Bending*(0.033)
Measured d_{max}	2.5	2.2	1.7

B. Skin Contact

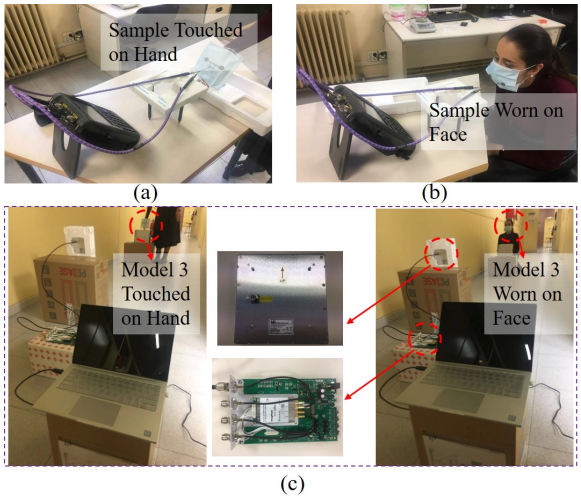

Fig. 16. Measurement setup for the impedance, reflection coefficients and read ranges in different skin contact positions. (a) Sample touched on a hand, (b) Sample worn on face, (c) Read range measurement

Skin contact test setup is shown in Fig. 16. The reflection coefficient and read range measurements of the Design 3 are operated when the sample is touched on a hand and worn on face as shown in Fig. 16(a) (b) and (c), respectively. The first application of surgical masks is to be worn on face, so the samples tested in air or touched on hands are compared with that worn on face. In general, the skin-contact performance is limited by the resonance frequency shift and reduced radiation efficiency due to the impedance change and power loss in the human body, respectively.

As shown in Fig. 17, compared with the impedance in air, the impedance on a hand has lower resistance part and reactance part while that on face has higher both parts. In addition, compared with the curves of the sample in air, the reflection coefficient ($|S_{11}|$) curves as shown in Fig. 18 on a hand and face show the resonance frequencies are shifted to 956 MHz and 813 MHz, respectively. However, when the sample are on a hand and face, the values at 868 MHz are -13 dB and -13.5 dB, respectively.

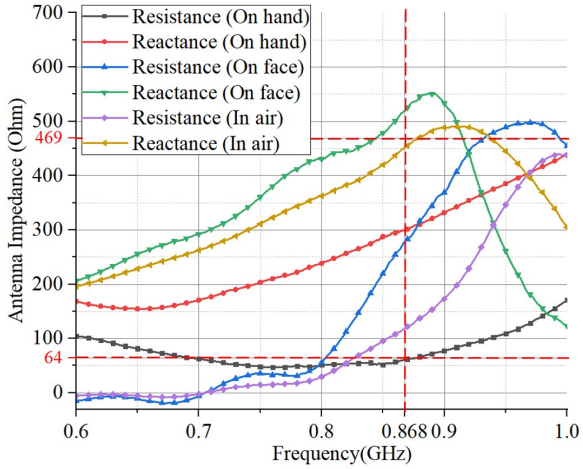

Fig. 17. Measured impedance in different skin contact positions (Dashed lines: required antenna complex impedance 64+i*469 ohm at 868 MHz).

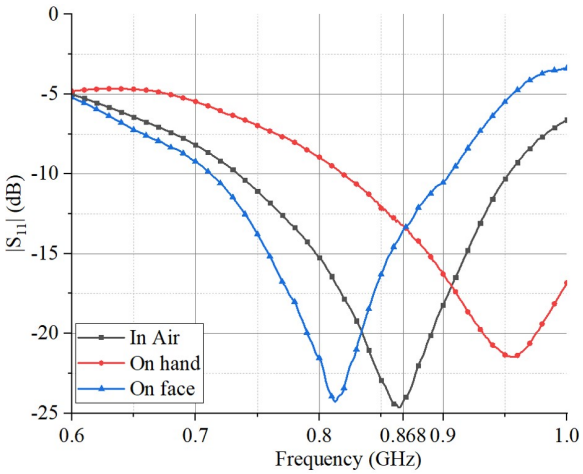

Fig. 18. Measured reflection coefficients in different skin contact positions.

TABLE IV
MEASURED MAXIMUM READ RANGE OF THE DESIGN 3 IN DIFFERENT SKIN CONTACT POSITIONS(UNIT: M)

Type	*InAir*	*On a Hand*	*On face*
Measured d_{max}	2.5	0.8	1.1

Read range tests in different situations are necessary and the results are shown in Table IV.The measured max values of the read ranges shown in Table IV are 2.5 m, 0.8 m and 1.1 m in air, on hand and on face, respectively. From the results, skin contact causes a decrease in read ranges and the minimum read range (1.1 m) when used on face proves that Design 3 can be effectively worn.

VI. Conclusion

To conclude, the progressive designs of textile UHF-RFID antennas on surgical masks are developed and one of them (Design 3) is selected to be validated by reliability tests (bending and skin contact). To explore the possibility and reliability of the function-extensible IC chips for textile UHF-RFID sensors, an IC chip (Rocky 100) with lower sensitivity (-10 dBm) than that of the popular chip (Monza R6, -20 dBm) is used in the designs. The simulated and measured resonance curves of the designs all match well (all below -20 dB at 868 MHz) and the radiation performance (realized gain) are improved progressively (maximum values: -10.86 dBi, -7.87 dBi and 1.09 dBi). After comparing the three progressive designs, the best type (Design 3) is selected and its read ranges measured by RFID reader (M6e kit) can reach 2.5 m in air. In addition, the necessary reliability validation measurements (bending and skin contact) are performed. From the results, the resonance frequency shift degrees are slightly different (all below 20 MHz) under different bending degrees (radius: 33 mm to flat) while heavily distinguishing on a hand (88 MHz) or face (55 MHz), but the values of reflection coefficients at 868 MHz all are below -10 dB. The maximum read range can reach 1.1 m on face. As a result, the proposed Design 3 has common use as an ID tag for tracking or safe distance alert in the epidemic situation but for the used function-extensible chip, the design can extend many different types of textile sensors for various application scenarios in the future.

References

[1] C. Occhiuzzi, C. Paggi and G. Marrocco, "Passive RFID Strain-Sensor Based on Meander-Line Antennas," *IEEE Trans. Antennas Propag.*, vol. 59, no. 12, pp. 4836-4840, Dec. 2011.

[2] C.Y. Luo, I. Gil and R. Fernández-García, "Wearable Textile UHF-RFID Sensors: A Systematic Review," *Materials*, vol. 13, no. 15, pp. 3292, 2020.

[3] M. Yang, Wen. Zhang, L. Li, L. Han, X. Chen, R. Yang and Q. Zeng, "A Resistance-Type Sensor Based on Chipless RFID," *IEEE Trans. Antennas Propag.*, vol. 65, no. 7, pp. 3319-3325, Jul. 2017.

[4] Y. Shafiq, J. S. Gibson, H. Kim, C. P. Ambulo, T. H. Ware and S. V. Georgakopoulos, "A Reusable Battery-Free RFID Temperature Sensor,"*IEEE Trans. Antennas Propag.*, vol. 67, no. 10, pp. 6612-6626, Oct. 2019.

[5] Y. Wang, A. J. Pretorius and A. M. Abbosh, "Low-Profile Antenna With Elevated Toroid-Shaped Radiation for On-Road Reader of RFID-Enabled Vehicle Registration Plate," *IEEE Trans. Antennas Propag.*, vol. 64, no. 4, pp. 1520-1525, Apr. 2016.

[6] Z. Ali, E. Perre, N. Barbot and R. Siragusa, "Authentication Using Metallic Inkjet-Printed Chipless RFID Tags," *IEEE Trans. Antennas Propag.*, vol. 68, no. 5, pp. 4137-4142, May. 2020.

[7] K. Kapucu and C. Dehollain, "A passive UHF RFID system with a low-power capacitive sensor interface," in *2014 IEEE RFID Technology and Applications Conference (RFID-TA)*, Tampere, 2014,pp. 301-305.

[8] K. Koski, L. Sydänheimo, Y. Rahmat-Samii and L. Ukkonen, "Fundamental Characteristics of Electro-Textiles in Wearable UHF RFID Patch Antennas for Body-Centric Sensing Systems," *IEEE Trans. Antennas Propag.*, vol. 62, no. 12, pp. 6454-6462, Dec. 2014.

[9] H. He, X. Chen, Z. Khan, L. Sydänheimo, L. Ukkonen,J. Li, H. Nishikawa and J. Virkki, "Textile-based Passive Sensor for Air Humidity," in *2020 IEEE 8th Electronics System-Integration Technology Conference (ESTC)*, Tønsberg, Vestfold, Norway, 2020, pp. 1-3.

[10] Y.Y. Fu, Y. Chan, M. Yang, Y. Chan and J. Virkki, "Experimental Study on the Washing Durability of Electro-Textile UHF RFID Tags," *IEEE Antennas Wirel. Propag. Lett.*, vol. 14, pp. 466-469, Nov. 2014.

[11] R.B.V.B. Simorangkir, D. Le, T. Björninen, A. S. M. Sayem, M. Zhadobov and R. Sauleau, "Washing Durability of PDMS-Conductive Fabric Composite: Realizing Washable UHF RFID Tags," *IEEE Antennas Wirel. Propag. Lett.*, vol. 18, no. 12, pp. 2572-2576, Dec. 2019

[12] S. Shao, A. Kiourti, R. J. Burkholder and J. L. Volakis, "Broadband Textile-Based Passive UHF RFID Tag Antenna for Elastic Material," *IEEE Antennas Wirel. Propag. Lett.*, vol. 14, pp. 1385-1388, Feb. 2015.

[13] D.P. Rose, M. E. Ratterman, D. K. Griffin, L. Hou, N. Kelley-Loughnane, R. R. Naik, J. A. Hagen, I. Papautsky and J. C. Heikenfeld, "Adhesive RFID Sensor Patch for Monitoring of Sweat Electrolytes," *IEEE. Trans. Biomed. Eng.*, vol. 62, no. 6, pp. 1457-1465, Jun. 2015.

[14] D. Patron, W. Mongan, T. P. Kurzweg, A. Fontecchio, G. Dion, E. K. Anday and K. R. Dandekar, "On the Use of Knitted Antennas and Inductively Coupled RFID Tags for Wearable Applications," *IEEE Trans. Biomed. Circuits Syst.* , vol. 10, no. 6, pp. 1047-1057, Dec. 2016.

[15] M. A. S. Tajin, A. S. Levitt, Y. Liu, C. E. Amanatides, C. L. Schauer,G. Dion, and K. R. Dandekar, "On the effect of sweat on sheet resistance of knitted conductive yarns in wearable antenna design," *IEEE Antennas Wirel. Propag. Lett.*, vol. 19, no. 4, pp. 542–546, Feb. 2020.

[16] Y. Liu, A. Levitt, C. Kara, C. Sahin, G. Dion, and K. R. Dandekar,"An improved design of wearable strain sensor based on knitted RFID technology," in *2016 IEEE Conference on Antenna Measurements Applications (CAMA)*, 2016, pp. 1–4.

[17] C. A. Balanis, Antenna Theory Analysis And Design, 3rd ed., John Wiley and Sons, 2005, pp.523–533.

[18] M. A. S. Tajin, O. Bshara, Y. Liu, A. Levitt, G. Dion, and K. R. Dandekar, "Efficiency measurement of the flexible on-body antenna at varying levels of stretch in a reverberation chamber," *IET Microw. Antennas Propag.*, Jul. 2019.

[19] M. Chesser, A. Jayatilaka, R. Visvanathan, C. Fumeaux, A. Sample and D. C. Ranasinghe, "Super Low Resolution RF Powered Accelerometers for Alerting on Hospitalized Patient Bed Exits," in *2019 IEEE International Conference on Pervasive Computing and Communications (PerCom)*, Kyoto, Japan, 2019, pp. 1-10

[20] L. Shan and H. Xiao, "Impedence characterization of RFID tag antennas and application in conformal tag antenna," in *2015 7th Asia-Pacific Conference on Environmental Electromagnetics (CEEM)*, Hangzhou, 2015, pp. 140-142

[21] H. Zhu, Y. C. A. Ko and T. T. Ye, "Impedance measurement for balanced UHF RFID tag antennas," in *2010 IEEE Radio and Wireless Symposium (RWS)*, New Orleans, LA, 2010, pp. 128-131

[22] X. Qing, C. K. Goh and Z. N. Chen, "Measurement of UHF RFID tag antenna impedance," in *2009 IEEE International Workshop on Antenna Technology*, Santa Monica, CA, 2009, pp. 1-4

[23] M. Svanda and M. Polivka, "Matching Technique for an On-Body Low-Profile Coupled-Patches UHF RFID Tag and for Sensor Antennas," *IEEE Trans. Antennas Propag.*, vol. 63, no. 5, pp. 2295-2301, May. 2015.

[24] K. Rasilainen, J. Ilvonen and V. Viikari, "Antenna Matching at Harmonic Frequencies to Complex Load Impedance," *IEEE Antennas Wirel. Propag. Lett.*, vol. 14, pp. 535-538, Nov. 2015.

[25] M. A. Richards, Fundamentals of Radar Signal Processing, 2nd ed., McGraw-Hill Education, 2005, pp.523–533.

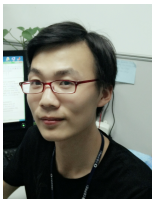

Chengyang Luo was born in Hubei, China, in 1995. He received the B. Eng. degree in integrated circuit design and integration system from Xidian University, Xi'an, China, in 2017. From 2019 to now, he is studying for the Electronics Engineering Ph.D. degree in Universitat Politecnica de Catalunya, Barcelona, Spain.

In 2017, he joined the China Electronic Product Reliability and Environmental Testing Research Institute (CEPREI), Guangzhou, China, where he served as a research assistant of the Science and Technology on Reliability Physics and Application of Electronic Component Laboratory, Guangzhou, China. In 2019, he obtained the national CSC-UPC Scholarship for the Ph.D. degree in Universitat Politecnica de Catalunya, Barcelona, Spain. His current research interests include textile UHF-RFID tags and sensing techniques, smart devices and noncontact voltage, current and power measurement techniques.

Ignacio Gil was born in 1978 in Barcelona, Spain. He received degrees in physics and electronics engineering in 2000 and 2003, and then his PhD in 2007 from the Universitat Autònoma de Barcelona, Spain. From 2003 to 2008 he was assistant professor in electronics and a researcher with the RF-Microwave Group in the Electronic Engineering Department, Universitat Autonòma de Barcelona, Spain. From 2006 to 2008 he worked for EPSON Europe Electronics GmbH where he developed high-performance integrated RF CMOS circuits, transceivers and system design. In 2008 he joined the Electronic Engineering Department, Universitat Politècnica de Catalunya (UPC), Spain, as lecturer and researcher. Since 2011 he is associate professor at UPC. Since 2012 he is also a collaborator at Universitat Oberta de Catalunya (UOC), Spain. He has been involved in 12 research projects (3 as principal researcher) in different research activities including passive and active RF and microwave devices and circuits, metamaterials, EMC and smart textile electronics. From 2012-2014 he served as Chairman of the Spanish IEEE EMC Chapter. In 2017 he was academic visitor at Loughborough University (UK) in the Wireless Communications Research Group. Since 2019 he is Deputy Director of International Relations at ESEIAAT (UPC). Dr. Gil is co-author of more than 150 scientific publications and 17 patents. He has been awarded the Duran Farell de Investigación Tecnológica (2006) and the patent award from SEIKO EPSON Corporation (2010). Dr. Gil has been visiting professor in different Universities: New Jersey Institute of Technology (USA), Limerick University (Ireland), Loughborough University (UK), Shaoxing University (China) and Polytechnic University of Tirana (Albania).

Raul Fernandez Garcia received the B.Eng. degree in telecommunications and M.Eng degree in electronics from the Universitat Politecnica de Catalunya, Barcelona, in 1997 and 1999, respectively. In 2007 he received the Ph.D. degree from the Universitat Autonoma de Barcelona. From 1998 to 2001, he worked for Sony Spain, as Radiofrequency Engineer, where he developed analog and digital TV tuners. From 2001 to 2007, he was part-time Assistant Professor in electronics with the Department of Electronics Engineering, Universitat Autonoma de Barcelona. Funded by the European Marie Curie Program, he worked on devices and circuits reliability at IMEC (Belgium) between 2005 and 2006. From 2008 to 2011, he was full-time Assistant Professor in the Department of Electronics Engineering, Universitat Politecnica de Catalunya. At present he is Associate Professor at the same department. Dr. Fernandez-Garcia is author or a co-author of more than 110 papers in international journals and conferences and he has been involved in 18 research projects (6 as principal researcher) in different research activities including reliability, electromagnetic compatibility and electronic textile. He was the recipient of Best Paper Awards at IPFA 2007. His current scientific interest is focused on wearable sensor development for sport and health applications.